AD-A115 937 CALIFORNIA UNIV SANTA BARBARA QUANTUM INST F/G 20/7
DESIGN OF THE UCSB FEL ELECTRON BEAM SYSTEM,(U)
OCT 81 L R ELIAS, G RAMIAN N00014-80-C-0308
UNCLASSIFIED QIFEL-011/81 NL

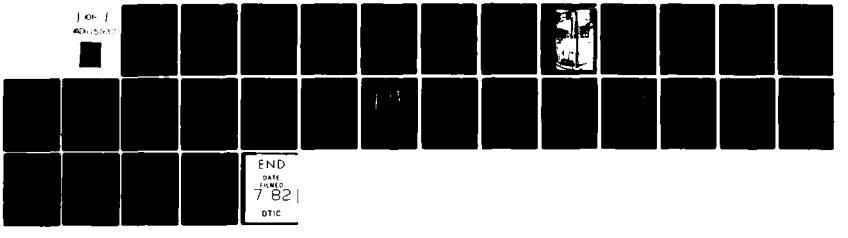

END
DATE FILMED
7 82
DTIC

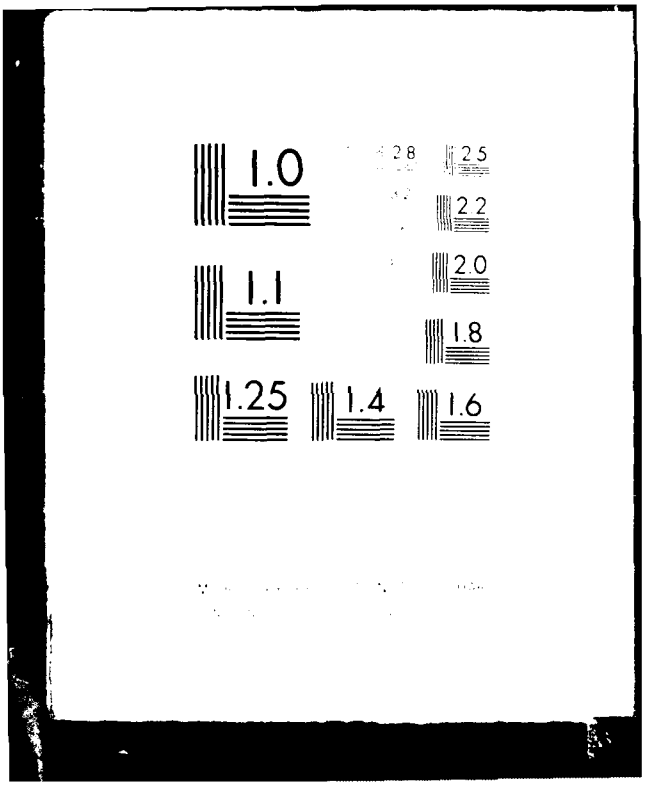
1.0
2.8
2.5
2.2
1.1
2.0
1.8
1.25
1.4
1.6

395-202

File Contracts reports (1)

AD A115937

Design of the UCSB FEL
Electron Beam System

Luis R. Elias and Gerald Ramian
Quantum Institute
University of California
Santa Barbara, California 93106
QIFEL011/81

OCTOBER 28, 1981

UNIVERSITY OF CALIFORNIA
SANTA BARBARA
QUANTUM INSTITUTE

FREE ELECTRON LASER PROJECT

DTIC
ELECTE
JUN 22 1982
S D
B

DISTRIBUTION STATEMENT A
Approved for public release;
Distribution Unlimited

DTIC COPY

82 05 2 168

Design of the UCSB FEL Electron Beam System

Luis R. Elias and Gerald Ramian
Quantum Institute
University of California
Santa Barbara, California 93106

Research supported by The Office of Naval Research and Air Force Office Of Scientific Research, Contract N00014-80-C-0308

INTRODUCTION

The UCSB FEL experimental program was initiated January 15, 1980 at the Quantum Institute of the University of California at Santa Barbara. It's principal objective is to demonstrate the operation of electrostatic-accelerator free-electron lasers in 1) the FIR-submillimeter region at high average power and high overall efficiency using a single stage FEL and 2) the visible-IR region with modest power and modest overall efficiency using a two-stage FEL. A discussion of the techniques used can be found in references 1, 2, and 3. A conceptual drawing of the UCSB FEL machine is shown in figure 1.

An important feature of the UCSB FEL is the recovery of the spent electron beam. Both 1) the average laser power and 2) the overall efficiency of the FEL increase with increased electron beam collection efficiency. Optimum laser performance can be

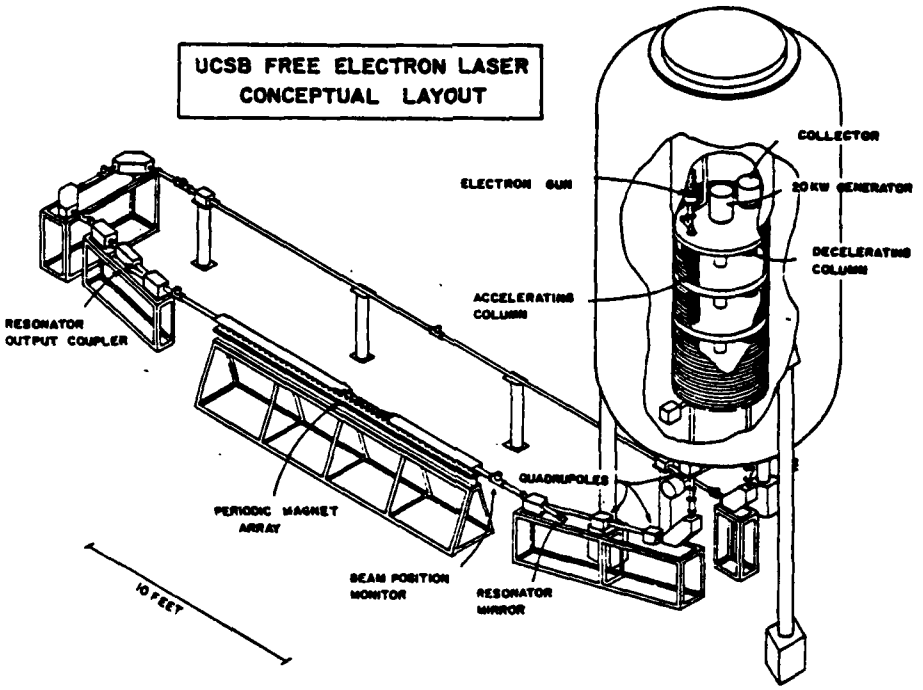

Figure 1.

achieved with this device provided only a small fraction of the total electric charge stored in the beam is lost while transporting it through the system.

Realization of this low charge loss condition can be achieved only if a very high quality electron beam can be produced and maintained throughout the electron accelerator and transport system. It is for this reason that a considerable amount of FEL project time has been dedicated to the design of a high quality electron beam source and an electron transport and recovery system having a minimum amount of optical aberrations.

The first phase of the UCSB FEL experiment deals solely with the construction and testing of a high-quality electron beam system with electron beam recovery, suitable to operate a

single-stage FEL in the submillimeter region. This report describes the design of the major portions of the system. In addition, results of experimental measurements of the electron beam quality at the exit of the electron gun are presented. The goal of this temporary design is to show that an electron beam can be produced and transported through the system with a minimum amount of charge losses. Although the collected beam in this phase of the experiment is a monochromatic beam, the electron beam optics has been designed to accept an electron beam whose phase-space has been modified by the future FEL interaction.

A description of the overall system hardware is first presented in the paper. Later, the design of each of the following major electron beam components of the system will be discussed in detail: 1) the electron gun, 2) the electron accelerator/decelerator 3) the external electron transport system, 4) the electron collector. Finally, a discussion of the main objectives of the electron recirculation tests is presented at the end.

DTIC COPY INSPECTED

Accession For
NTIS GRA&I
DTIC TAB
Unannounced
Justification
PER LETTER
Distribution/
Availability Codes
Dist Avail and/or Special
A

EXPERIMENTAL HARDWARE

The present configuration of the UCSB FEL electron beam system is illustrated in figures 2 and 3. For lack of space the two figures are presented separately from one another, but they should be viewed as a single drawing with figure 2 laying on top of figure 3. Figure 2 shows the important components of the electron beam system inside the vertically standing electrostatic accelerator tank. The accelerator is presently located at the National Electrostatic Corporation manufacturing plant in Middleton, Wisconsin. The dome-shaped structure shown on top of figure 1 represents the high-voltage terminal of the system. Using pelletron chains the H.V. terminal can be charged to a maximum of -3MV with respect to tank potential. The terminal voltage is controlled by the corona triode shown on top of the terminal shell. On a steady basis the terminal voltage is a function of the amount of corona discharge to ground produced by the triode. In conjunction with a beam energy sensor (not shown) the corona triode is capable of maintaining the voltage stability of the terminal to within one part in 10,000 for long periods of time. The terminal shell houses the electron gun, the electron collector, the permanent magnet generators and other electronic components. The two permanent magnet generators are capable of providing 20 KVA of 800 Hz electrical power. The generators are driven by the rotating plastic shaft shown in the figure. The shaft is driven itself by a 30 hp motor located at

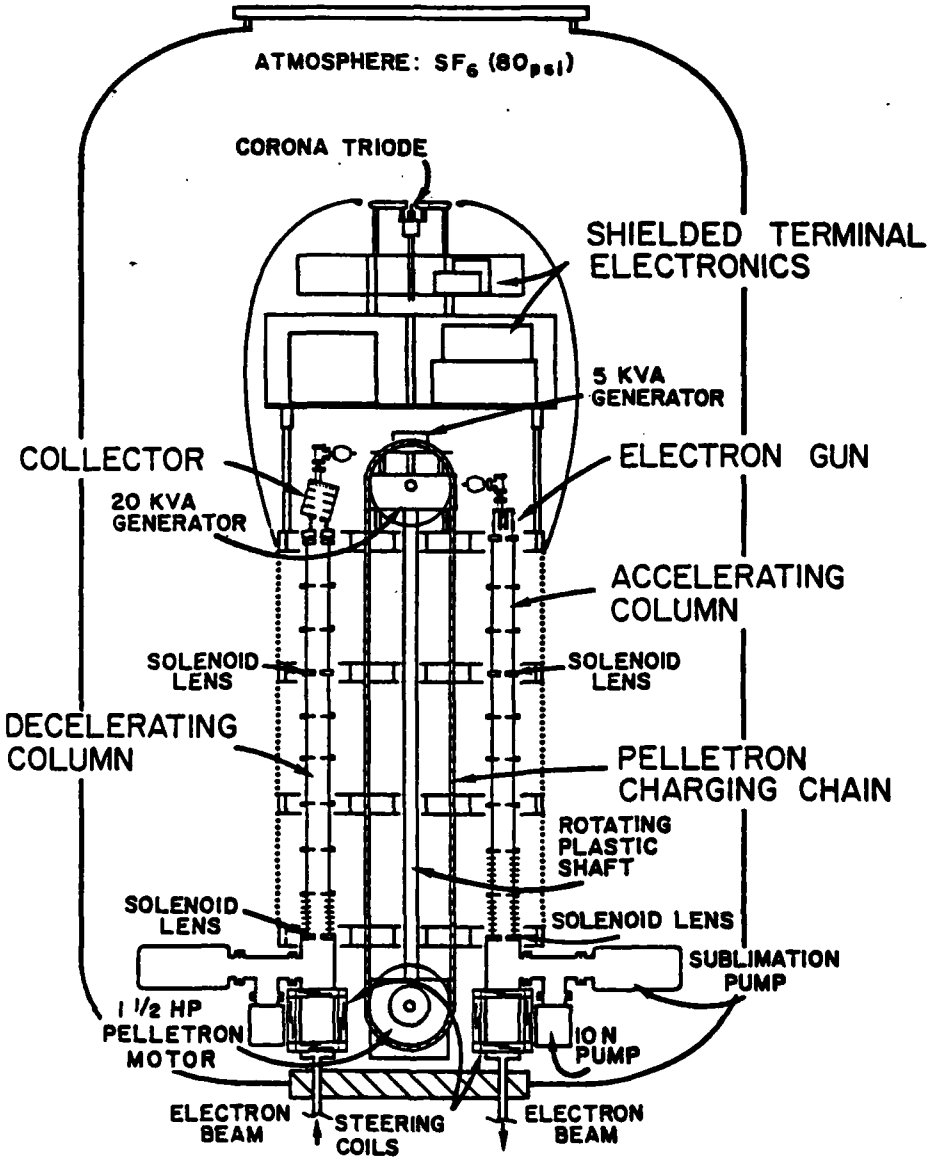
ATMOSPHERE: SF_6 (80 psi)
CORONA TRIODE
SHIELDED TERMINAL ELECTRONICS
5 KVA GENERATOR
COLLECTOR
ELECTRON GUN
20 KVA GENERATOR
ACCELERATING COLUMN
SOLENOID LENS
SOLENOID LENS
DECELERATING COLUMN
PELLETRON CHARGING CHAIN
ROTATING PLASTIC SHAFT
SOLENOID LENS
SOLENOID LENS
SUBLIMATION PUMP
1 1/2 HP PELLETRON MOTOR
ION PUMP
ELECTRON BEAM
STEERING COILS
ELECTRON BEAM

Figure 2.

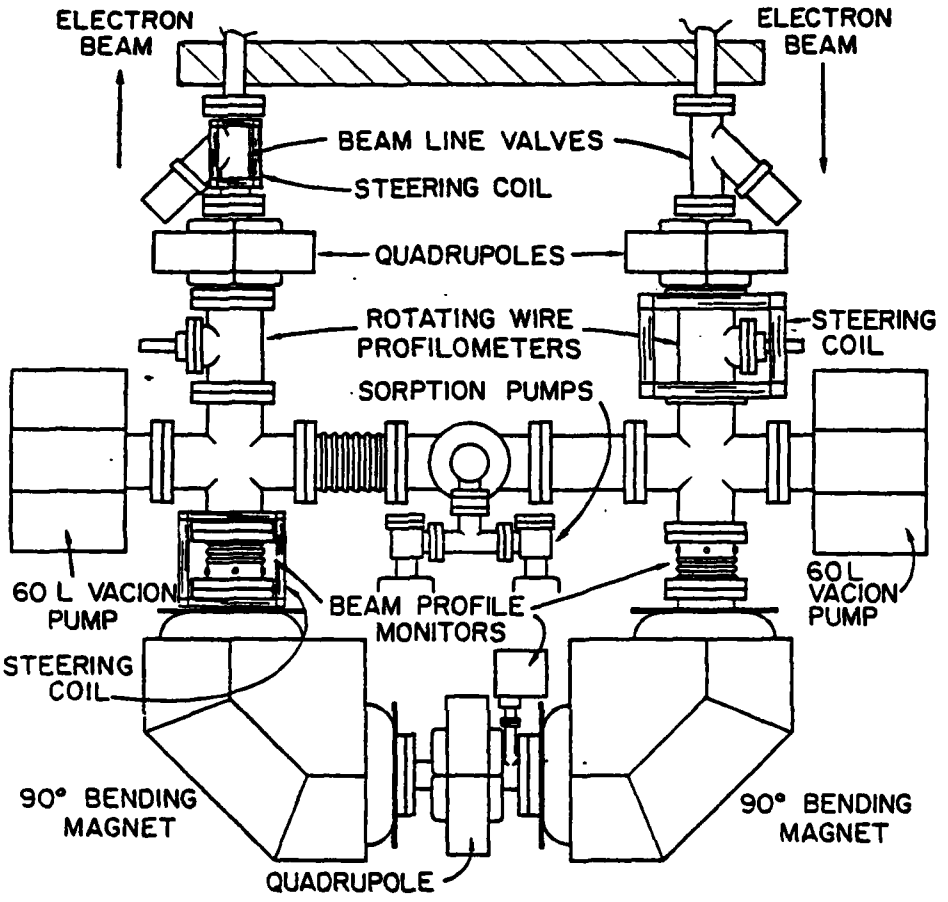

Figure 3.

the bottom of the tank, next to the vacuum pumps and next to the 1-1/2 hp pelletron chain motor. A photograph of the HV terminal prior to installation is shown in figure 4.

Two-way communication between the high voltage terminal and control console is achieved by means of 16 optical links running vertically up and parallel to the accelerator tubes. Complete remote control of anode to cathode voltage, filament power, aperture grid voltage and pulse length is thus available for the electron gun. Similarly, there is control over the

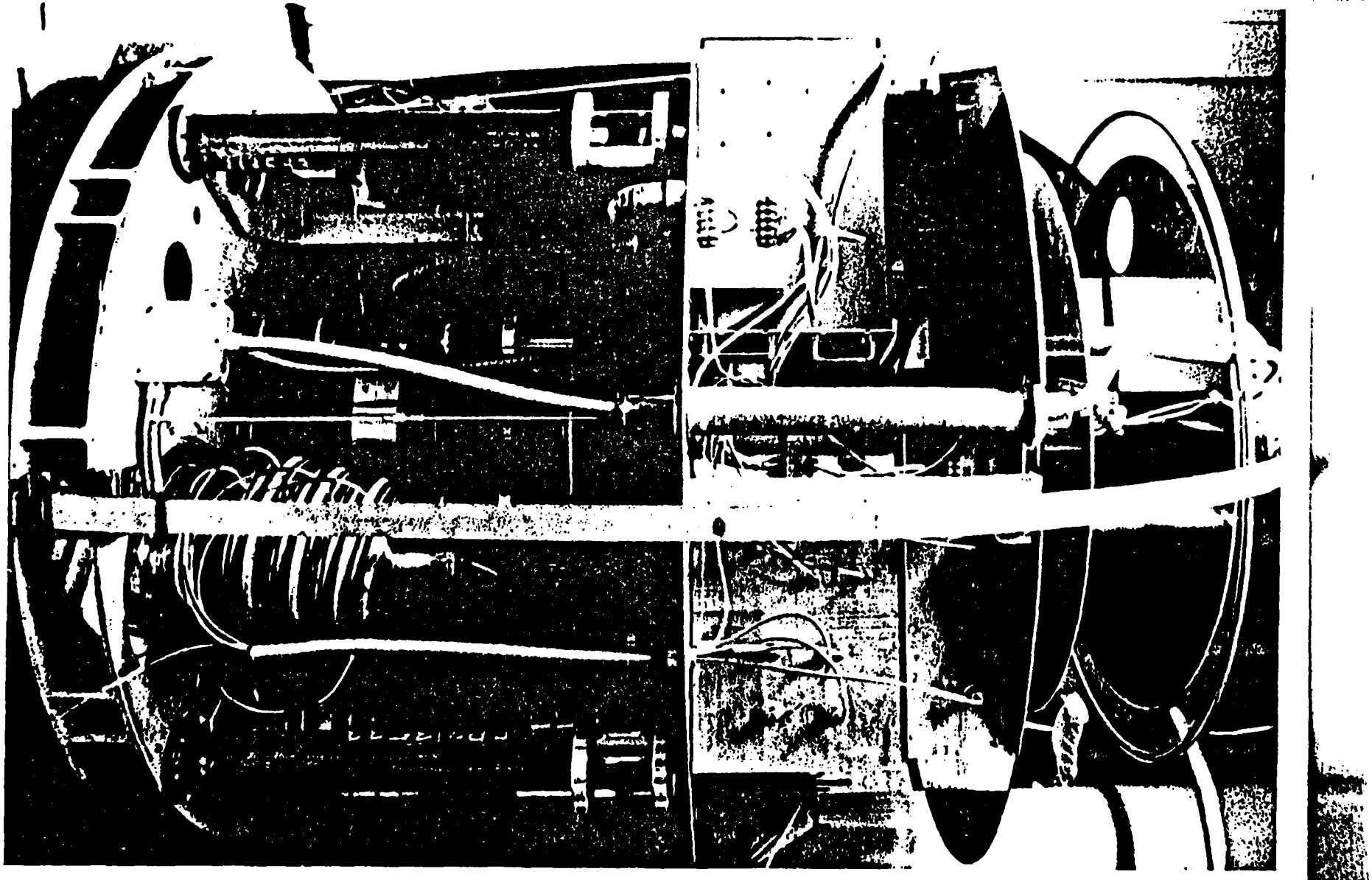

Figure 4.

voltage and focussing properties of the electron collector system. This feature will allow using the electron collector as an electron energy spectrometer when the FEL portion of the experiment is implemented later. Furthermore, the optical links allow monitoring of various signals inside the HV terminal such as: a) gun cathode current, b) gun anode current, c) electron current recovered by each of four electron collector plates, and f) terminal temperature.

Below the HV terminal two accelerating columns are shown. They are each composed of nine standard ceramic accelerator sections manufactured by National Electrostatic Corporation. With the accelerator charged to -3MV the average electric field gradient along the accelerator column axis is 16 KV/cm. The accelerator column shown on the left hand side of figure 2 acts as a decelerating column for electrons injected upward at the bottom of the column. The total length of the accelerator/decelerator column is 183cm. It will accept an electron beam 1" in diameter.

At the bottom of each accelerator column and at two thirds its height, compact solenoid lenses have been installed to control the radius of the electron beam inside the accelerator and decelerator columns. Also, just below the solenoid lenses a set of x-y steering coils have been installed over each beam-line.

The external beam optics and electron beam diagnostic

components are shown schematically in figure 3. The beam optics design is an achromatic design consisting of two magnetic dipoles and three magnetic quadrupoles located as shown in the figure. A detail analysis of particle trajectories will be discussed later.

To measure electron beam positions and beam profile, three wire profilometers have been included in the design. In each profilometer a thin wire moves through the electron beam and scatters electrons. The transverse density of electrons in the beam is proportional to the collected current of scattered electrons. In addition to the wire profilometers, two beam position monitors have been installed as shown in the figure. Each consists of a four-quadrant cylindrical electrode with the electron beam moving parallel to the cylinder axis. The amount of charge induced by the electron beam on each plate is proportional to its distance from the plate. This means of measuring non-destructively beam positions will be used when complete electron beam storage is achieved.

At the bottom of the accelerated electron beam-line a Faraday cup has been installed to measure directly the electron beam current produced by the accelerator section.

ELECTRON GUN. The electrical design study of the gun was carried out by W.B. Herrmannsfeldt. The mechanical portion of the gun design was done by R. Hechtel and R. Van Iderstein. Four major constraints were imposed on the design of the electron gun. The first one was dictated by the FEL's requirements of sufficient electron beam current to obtain moderate small-signal laser gain ($g \sim 50\%$) in the submillimeter region with a single-stage FEL device. This constraint translated into an electron beam requirement of 2 amperes. The second constraint imposed required that the beam have the highest possible optical quality in order to 1) transport the electron beam with minimum charge loss throughout the FEL/accelerator/recovery system and 2) meet the beam quality requirements imposed by the FEL. To meet this constraint it was decided not to use a gridded cathode. The third constraint required that the electron gun have the ability to operate in a pulsed mode. To meet simultaneously constraints 2 and 3 an intermediate aperture-grid electrode was implemented into the design. The fourth constraint imposed on the gun design was that the electron beam produced by the gun be matched to the electron beam optics of the electrostatic accelerator tube in order to optimize beam transmission through it. This constraint required that the electron beam current injected into the accelerator have low divergence and a maximum radius of 12.5mm. The final gun design incorporated the use of a commercial planar oxide cathode 0.6" diameter operating at a cathode loading of

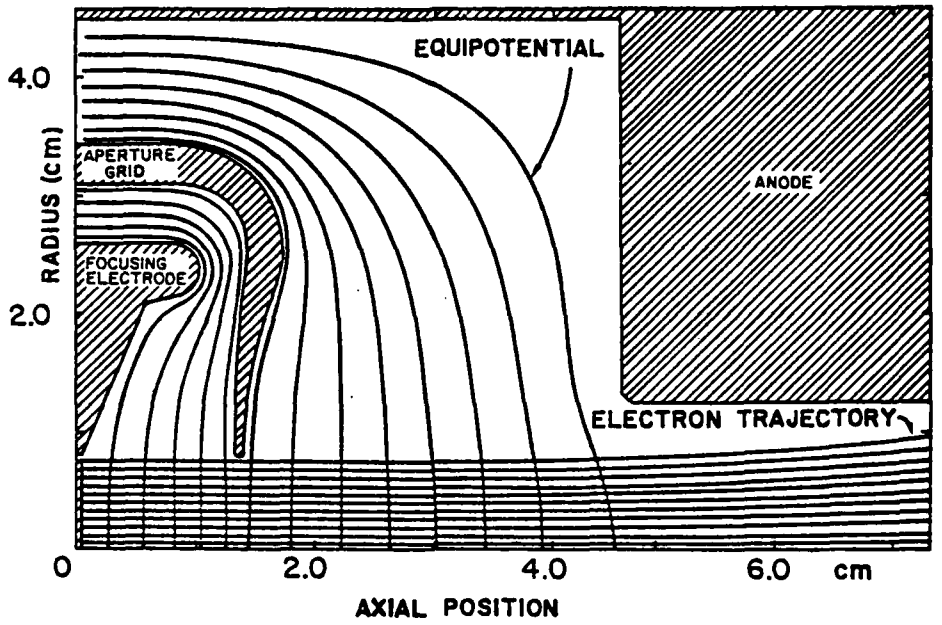

Figure 5.

about 1 ampere per cm^2.

The electrical design of the electron gun is shown in figure 5. Anode voltage is 50KV w.r.t.c. To turn on the electron beam, an aperture-grid voltage of 10KV w.r.t.c. is required. Under this condition the gun perveance is Ko = 0.217 μ-perv. To turn off the electron gun completely, a negative aperture-grid voltage of -2KV is needed. A drawing of the mechanical appearance of the electron gun is shown in figure 6 and a photograph of the assembled electron-gun is shown in figure 7. The construction and testing of the gun were carried out respectively by Hughes Aircraft Corporation at the Malibu Research Division, Malibu, California and at the Electron Beam Diagnostic Division at Torrance, California.

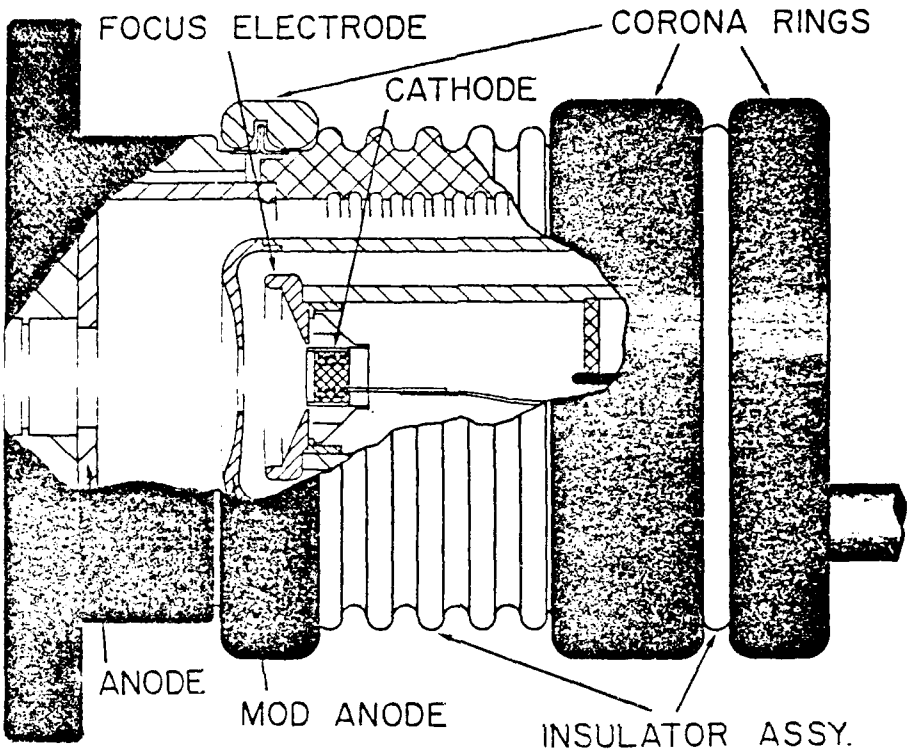

Figure 6.

To test the performance of the electron-gun a standard Hughes gun analyser was used. It consists of a probe with a small electron collecting aperture which is moved across the electron beam mapping the electron charge density over a plane perpendicular to the electron gun axis. A series of electron beam density profiles were obtained at various distances from the gun anode. In figure 8 the half width at half-maximum of each density profile has been plotted as a function of axial distance from the gun anode. The data has been reduced by R. Hechtel in order to calculate the transverse emittance of the electron beam. Within the resolution of the Hughes gun analyser probe the

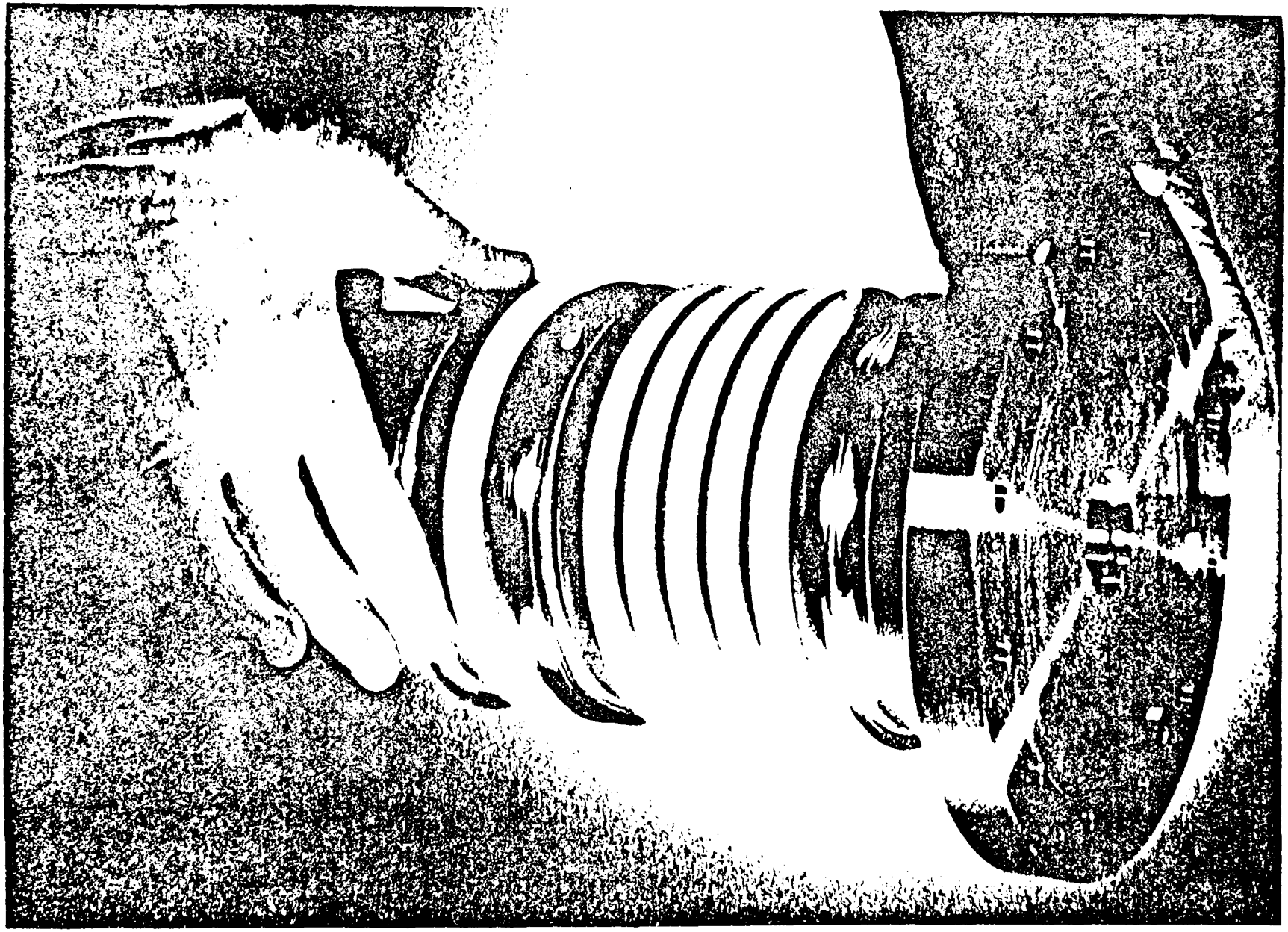

Figure 7

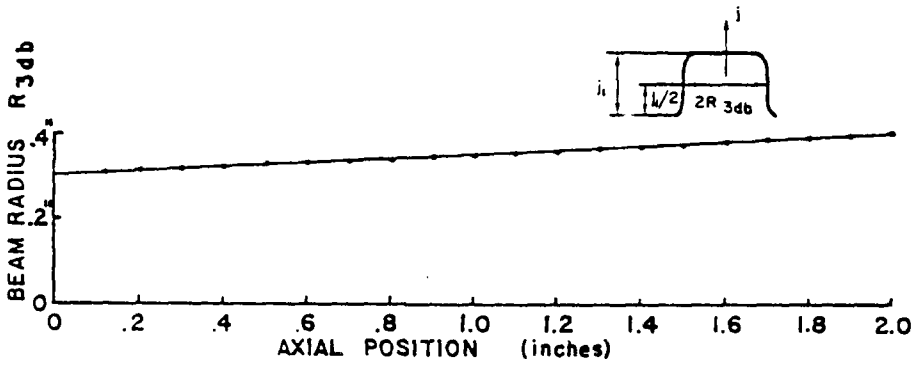

Figure 8.

calculation indicated that the electron gun has zero transverse emittance. Based on this measurement the transverse emittance of the UCSB electron gun is expected to have a value smaller than 1mm-mrad at 10KV. More accurate measurements of the transverse emittance of the electron gun will be made later. It is worth noting that the computer analysis of the electon beam yielded very nearly zero transverse emittance also, if thermal contributions are not included.

ELECTRON ACCELERATOR. The accelerator column consists of nine standard NEC accelerating tube sections, each approximately 20cm long separated by decoupling units containing a thin diaphragm with a 2.57cm aperture. Each tube section is made of alumina ceramic rings 1.3cm long separated by flat titanium rings. The voltage of each titanium ring and diaphragm is set by corona discharge currents. The electric fields produced inside each accelerator section change with position along the axis. The axial component of the electric field for the first accelerator section is plotted as a function of axial position in figure 9. The field reaches a maximum field of about 2.25MV/m half-way along the tube and drops to lower values at the position of the diaphragms. The variations in axial field with axial position gives rise to a transverse electric field. The effect of this field is to focus the electron beam.

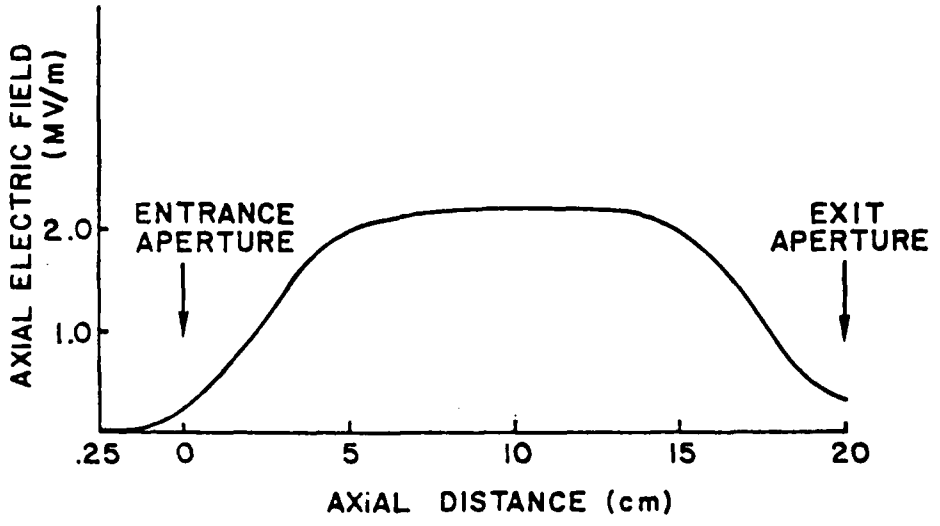

Figure 9.

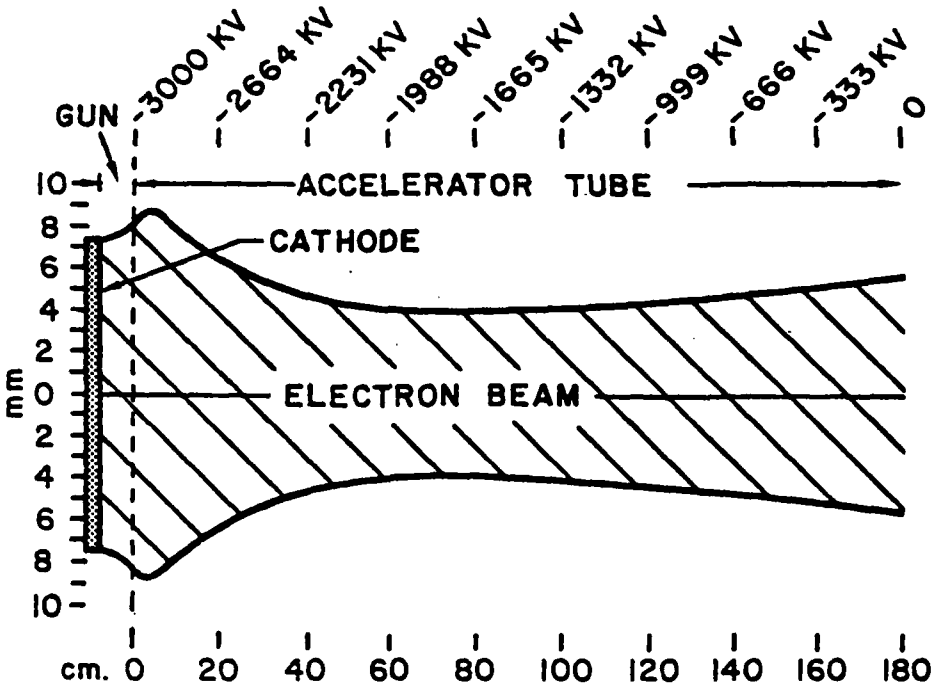

Figure 10.

To trace the trajectories of electrons along the accelerator tube a program has been written at UCSB that solves Laplace's electrostatic equations inside the accelerating tube. This information was used to determine the evolution of the envelope of the electron beam by solving numerically the Lorentz force equations[4] including self-field forces. A plot of the radius of the beam along the axis of the accelerator column is shown in figure 10. The initial radius and beam slope used were obtained from the experimental data shown in figure 8. It can be seen from figure 10 that due to a net outward radial force (i.e., space-charge force) the beam initially diverges fast but under the influence of the focussing fields of the accelerator column

the beam reaches a maximum radius of about 9mm just beyond the portion of the first diaphragm and then focusses to a mimimum radius of about 4mm half-way along the accelerator column. Although there is a focussing field at each of nine diaphragms equally spaced along the accelerator tube, only the first diaphragm has a noticeable effective focussing effect on the beam as shown in the figure. One reason for this is that after acceleration in the first section, the electrons have acquired relativistic speeds and the increased self magnetic-field force counteract almost completely the Coulomb space charge forces. The electron beam exits the accelerator column with a radius of about 6mm and a slope of about 3 milliradians.

Computer simulation of electron trajectories along the decelerator column show results very similar to those obtained in the accelerator column. It was found that at the entrance to the decelerator column the optimum convergence angle for the beam was about 3 milliradians at a radius of 6mm. For a non-monochromatic electron beam (e.g. $\Delta\gamma/\gamma \approx 0.2\%$) the trajectories of the electrons inside the decelerator column were nearly the same as that shown in figure 10. The only differences appeared at the end of the decelerator column near the electron collector. As shown in figure 2 there are four solenoid electron lenses located along the accelerator and decelerator columns. These lenses have been installed in order to make small corrections of beam radius and slope about their design values.

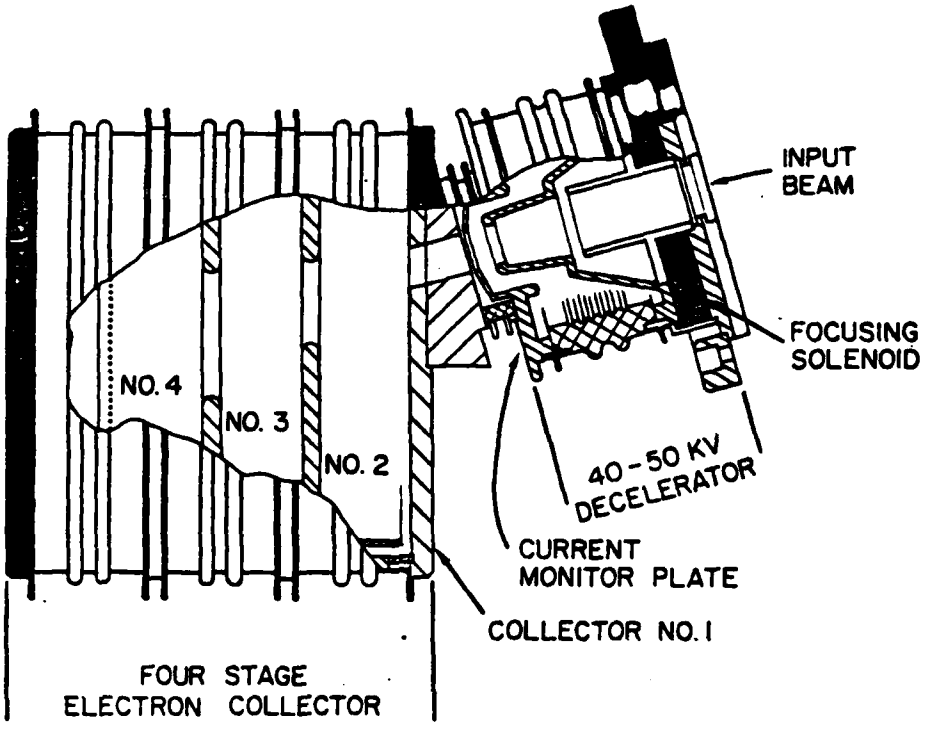

Figure 11.

ELECTRON COLLECTOR. The design of the UCSB FEL electron collector was carried out by Richard Hechtel. There are two distinct components in the electron collector system as shown in figure 11. There is a transition region which removes an amount of kinetic energy from the beam equal to that of the slowest moving electron. Also the transition region matches the electron beam optics between the decelerator column and the actual electron collector. The collector transition region has been designed to accept an electron beam 1) with maximum and minimum kinetic energy of 50kv and 40kv respectively and 2) with a ratio of RMS transverse electron velocity Vrms to axial electron

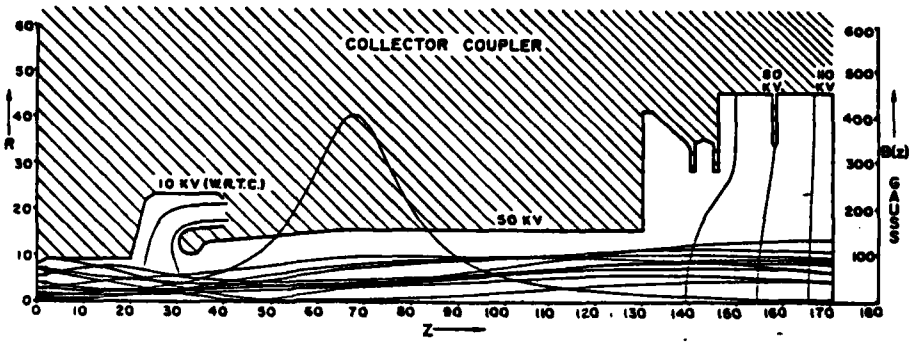

Figure 12.

velocity V_z of $Vrms/V_z=0.030$. To achieve this design a computer electron trajectory program was used. It included electron beam self forces and forces produced by external charged electrodes and that of a focussing solenoid. The resulting electrode trajectories are shown in figure 12. As shown in the figure, the trajectories were initiated well inside the last section of the decelerating column and terminated at the entrance of the actual electron collector. Three electron focussing regions are evident from the figure: 1) at the exit of the accelerator column, 2) at the region of varying magnetic field and 3) at the end of the transition region where electrode shapes and voltages have been designed to produce the desired focussing effects. The idea here is to counteract beam spreading forces produced by space charge and beam transverse emitance, and to transport and decelerate the beam between decelerator column and electron collector with a minimum amount of charge losses.

The actual electron collector unit is shown to the left of

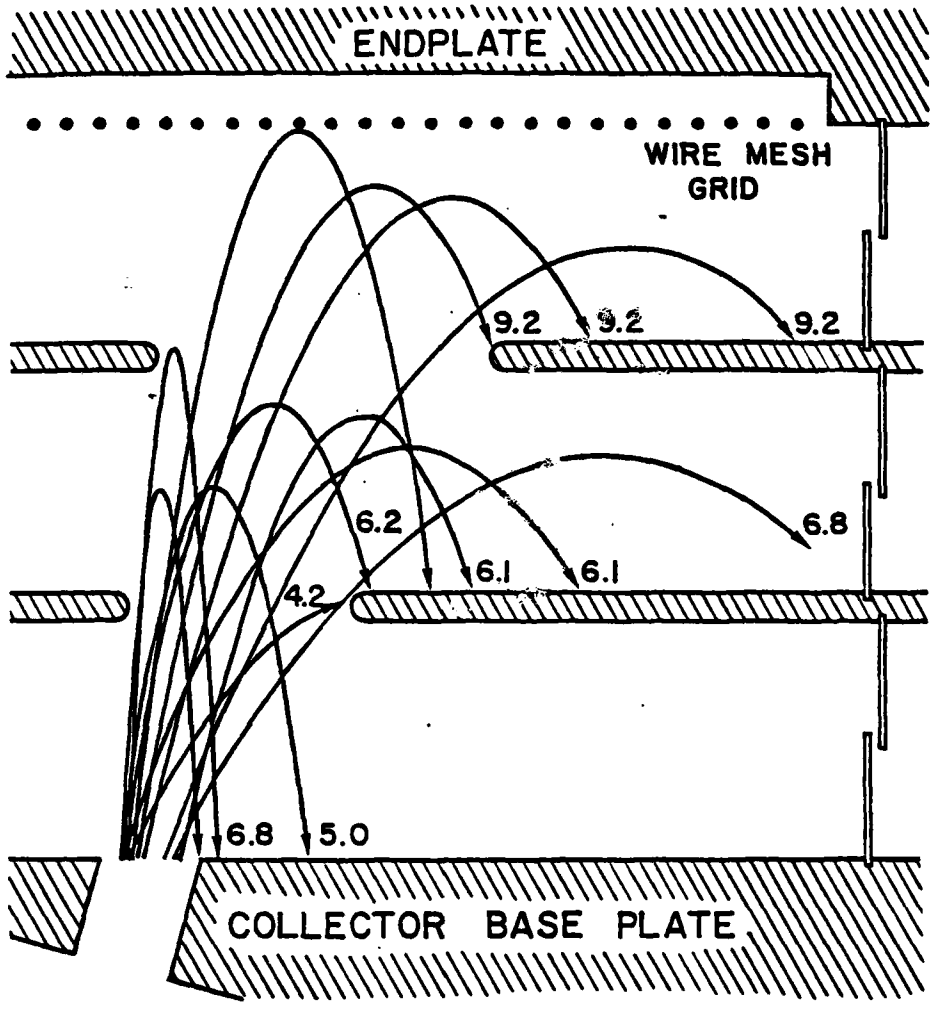

Figure 13.

figure 11. It consists of 4 collecting plates located with their planes making an angle of 15 degrees with respect to the axis of the transition region. This angle was chosen to minimize the possibility of electrons being reflected by the electrostatic fields inside the collector. A plot of some of the electron trajectories inside the collector is shown in figure 13. The highest energy trajectories have initial kinetic energy of 10KV,

and maximum V_{rms}/V_z=0.250. The maximum beam current acceptable to the collector system is 2 amperes.

The collector was assembled at the High Energy Physics Laboratory at Stanford University. The collector can be seen assembled in position inside the H.V. terminal shown in figure 4.

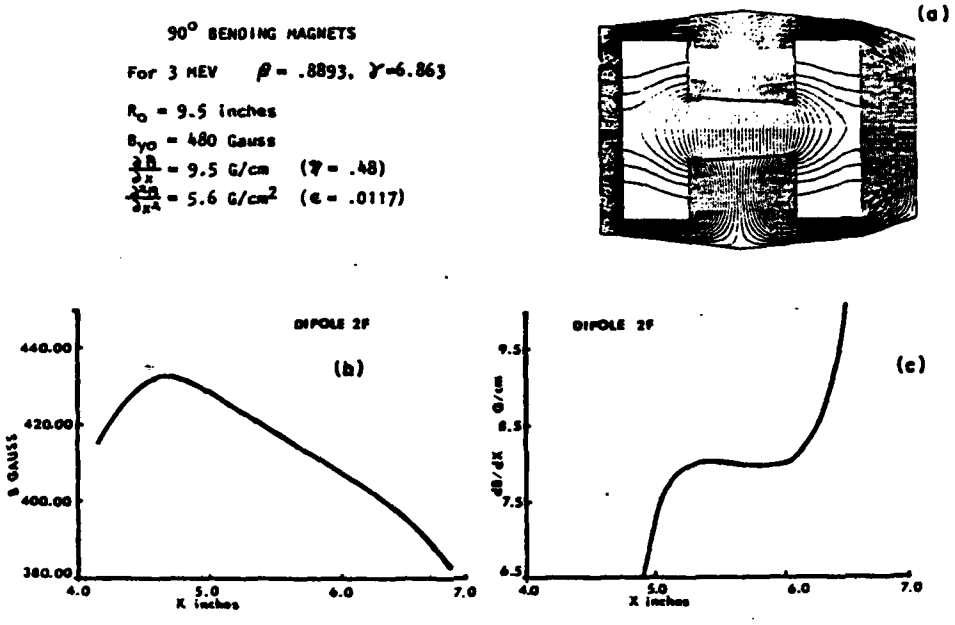

Figure 14.

EXTERNAL ELECTRON TRANSPORT SYSTEM. As noted earlier, to guarantee successful electron beam recovery it is important to have a high electron beam optical quality throughout the electron accelerator/transport system. With this constraint in mind a compact electron transport system has been designed for the electron recovery experiment. It consists basically of an achromatic 180° bend with three magnetic quadrupoles and two magnetic dipoles located as shown in figure 3. In addition, two solenoids located at the bottom of the accelerator tubes provide beam angle matching between accelerator tubes and the optical transport system external to the accelerator tank. The quadrupoles and dipoles were designed and assembled at UCSB. A

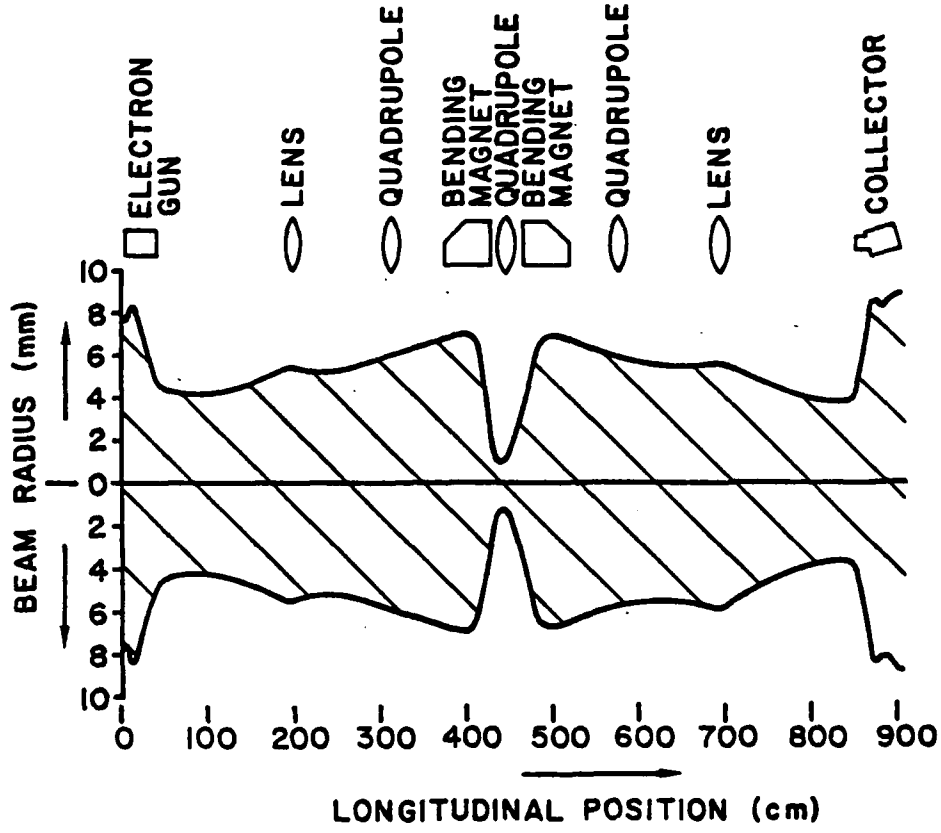

Figure 15.

plot of the design fields of the dipoles is shown in figure 14. They were obtained using the Poisson program. Figure 14a shows a plot of magnetic flux lines on a plane perpendicular to the motion of the electrons. The stepped pole faces allow for the linearization of the transverse field gradient without resorting to expensive curved machined surfaces. The value obtained is $d^2B/dx^2 = -0.125$ gauss/cm^2 over $\pm$1cm. Figure 14b and 14c show respectively the field B as a function of transverse position x and the field gradient dB/dx as a fuction of x. A sextupole

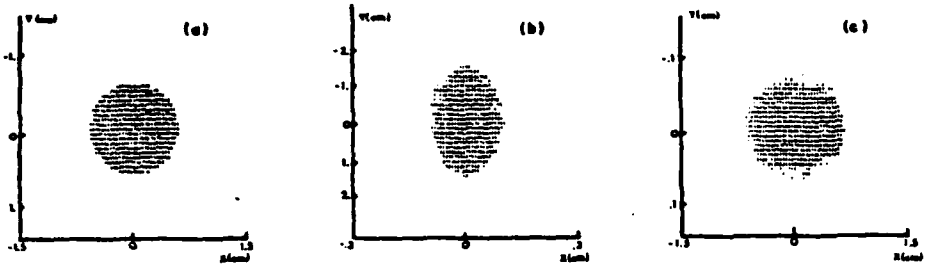

Figure 16.

component is provided by both a 1 inch long shaped pole-face section and by a radiused pole end piece. Mirror plates located 5cm from each end terminate the end fringe field. The coils can handle sufficient current for 10MeV operation.

Using the NAL TURTLE ray tracing program and the SLAC TRANSPORT program the transport properties of the 180° bend has been completely characterized. Figure 15 shows the calculated beam radius as a function of position along the external transport system as well as along the accelerator's internal optical components. This plot shows how the electron beam optics is matched through out the system. Figure 16 shows plots of transverse beam charge distribution at three positions along the external beam optics. Figure 16a, b, and c show, respectively, charge density distributions at a) the output of the accelerator tube, b) half-way between the dipoles and c) at the entrance to the accelerator column. 3000 rays were randomly chosen to fill a 10π mm-mr initial phase-space. Also, an electron energy spread $\Delta\gamma/\gamma=1\%$ was included. The Turtle program directly integrates the

equations of motion through the beam line elements and therefore takes into consideration aberrations of all order including cumulative effects. The excellent fidelity of the system indicated by plot 16c can be largely attributed to the high degree of symmetry of the system. The actual output beam is not expected to be as good since small misalignments and stray fields can introduce additional aberrations.

ELECTRON RECIRCULATION TEST OBJECTIVES.

The main objective of the electron recirculation test is to demonstrate that a 2 ampere, 3 MV, high optical quality electron beam can be stored using electrostatic accelerators. Under normal operation (no beam recovery) the UCSB electrostatic accelerator can be charged at a maximum rate of 500μa. This means that on a steady state basis it can produce a maximum beam current of 500μa. If 2 amperes of beam current is extracted from the accelerator the terminal voltage will drop at a rate of 10 KV/μsec due to the finite capacitance of the terminal ($C \approx 2 \times 10^{-10}$ farad). However, if a fraction δ of the electron beam is collected in the terminal through the decelerating section then the net discharge rate of the terminal voltage will be reduced to $(1-\delta) \times 10$KV/μsec. For complete charge recovery ($\delta = 1$) there is no voltage drop and the accelerator can be operated on a steady state basis at 2 amperes. However, for $\delta < 1$ the accelerator will have to be operated on a pulsed basis as described in reference 1. The initial goal of the electron recirculation test is to pulse the electron gun for a period of 100μsec at a 10HZ repetition rate. Then, as the recovery of the electron beam becomes more effective, the beam duty cycle will be increased by increasing the gun-on pulse length.

Figure 17 illustrates the expected power and current budget for the second phase of the experiment (i.e. with an FEL oscillator). The single stage FEL oscillator tests are expected

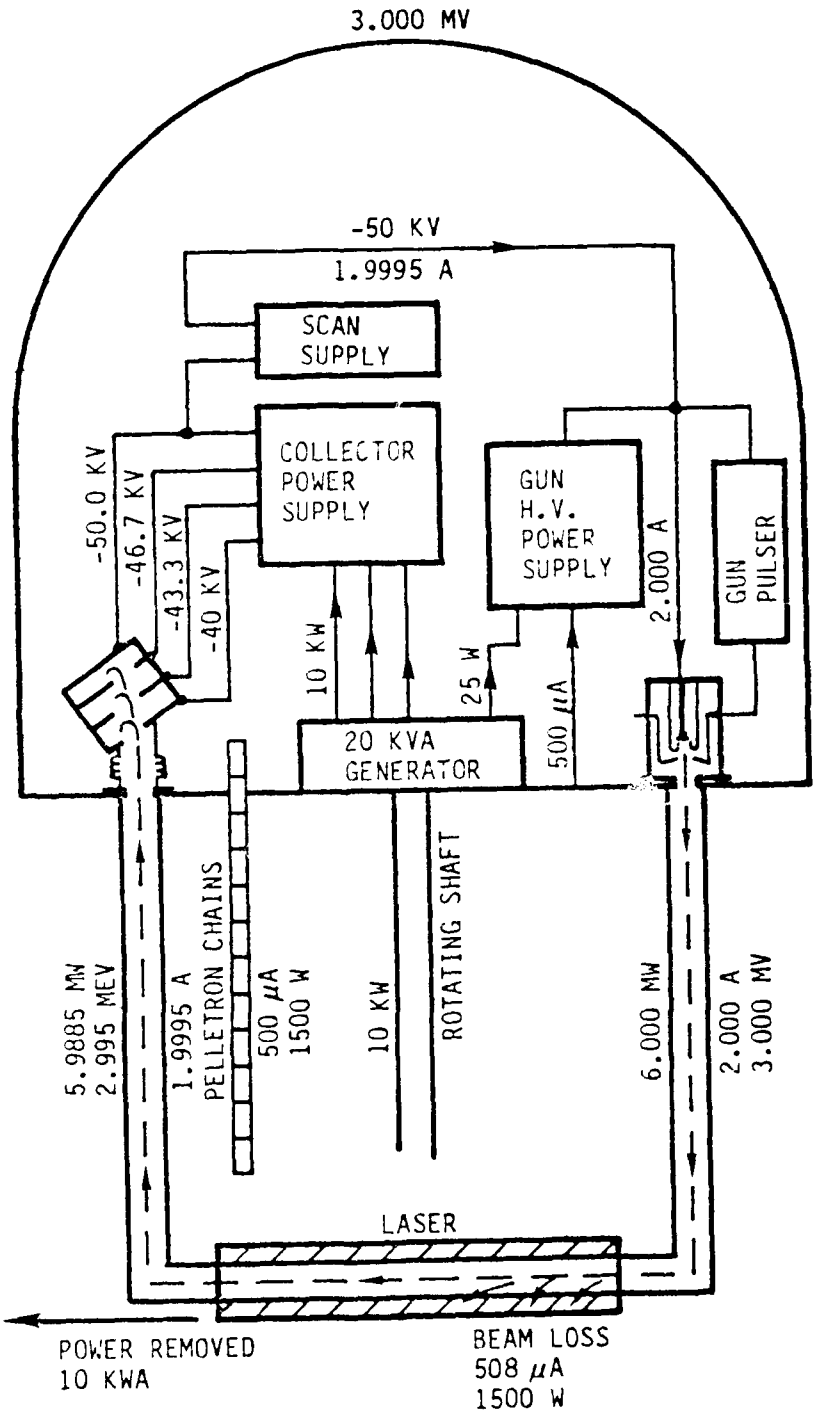
3.000 MV
-50 KV
1.9995 A
SCAN SUPPLY
COLLECTOR POWER SUPPLY
GUN H.V. POWER SUPPLY
GUN PULSER
-50.0 KV
-46.7 KV
-43.3 KV
-40 KV
10 KW
25 W
500 μA
2.000 A
20 KVA GENERATOR
5.9885 MW
2.995 MEV
1.9995 A
PELLETRON CHAINS
500 μA
1500 W
10 KW
ROTATING SHAFT
6.000 MW
2.000 A
3.000 MV
LASER
POWER REMOVED
10 KWA
BEAM LOSS
508 μA
1500 W

Figure 17.

to take place sometime in February of 1982.

The recirculation tests are presently being conducted at the National Electrostatic Corporation factory with the help of J. Ferry, R. Herb, and technical personnel. The authors wish to thank them for their colaboration. Also, we wish to thank P. Hayter, R. Whited, and M. Lowenstein for their help at UCSB.

REFERENCES.

1. "High-Power, cw, Efficient, Tunable (uv Through ir) Free-Electron Laser Using Low-Energy Electron Beams", Luis R. Elias, Phys. Rev. Letters, 42, 15, April 9, 1979.

2. "Electrostatic Accelerator Free Electron Lasers", QIFEL005/80 Report, Luis R. Elias, University of California, Quantum Institute, 1980; also published as a chapter in PHYSICS AND TECHNOLOGY OF FREE ELECTRON LASERS, Plenum Press, in press.

3. "The UCSB FEL Experimental Program",QIFEL006/80 Report, Luis R. Elias, University of California, Quantum Institute, 1980; also published as a chapter in PHYSICS AND TECHNOLOGY OF FREE ELECTRON LASERS, Plenum Press, in press.

4. "Magnetic Focusing of Electron Beams in the Presence of Transverse Velocity Components", J. Richard Hechtel, IEEE Transactions on Electron Devices, Vol. ED-28, 5, May 1981


DATE
FILME
7-8